IEICE TRANS. COMMUN., VOL.E78-B, NO.12 DECEMBER 1995

PAPER Special Issue on Satellite Remote Sensing

Polarimetric Enhancement in Radar Channel Imagery

Yoshio YAMAGUCHI†, *Member*, Yuji TAKAYANAGI†, *Student Member*, Wolfgang -M. BOERNER††, Hyo Joon EOM†††, *and* Masakazu SENGOKU†, *Members*

SUMMARY This paper applied the polarimetric filtering principle to Synthetic Aperture Radar (SAR) image sets in three possible polarimetric radar channels and compared the resultant imagery. The polarimetric radar channels in consideration here are Co-Pol, Cross (X)-pol, and Matched (M)-pol channels. Each channel has its own polarimetric characteristics for imaging. Using the formulation of the contrast enhancement factors based on the Stokes vector formalism, polarimetric enhanced images for three channels are shown using NASA JPL DC-8 AIRSAR data sets (CC0045L, Bonanza Creek, AK/USA). It is shown that the optimally enhanced Co- and X-Pol channel images play a decisive role in imaging in a complex featured background.

key words: *radio applications, polarimetry, SAR*

1. Introduction

Radar polarimetry, i.e., the full utilization of the electromagnetic vector wave information, has become an indispensable tool in modern radar and imaging technology [1]-[4]. Polarimetric imaging (polarization filtering) has been carried out by many investigators. Boerner's group (Kostinski, et al. [5]-[7], Tanaka, et al. [8]-[9]) have founded the polarimetric-filtering principle for both coherent and incoherent cases using the polarization ratio and the Stokes vector formulations. The CAL-TECH/JPL (NASA) group (van Zyl et al. [10]-[11]) applied the principle based on the Stokes vector formulation to the imaging of polarimetric Synthetic Aperture Radar (SAR) data acquired at NASA JPL. Touzi [12] proposed a filtering technique for SAR images for reducing speckle. Swartz et al. [13] solved the problem by using a decision-theoretic covariance matrix approach.

Although many approaches are available for polarization filtering, all of them use a distinct radar channel formulation, i.e., either the Matched (M)-Polarization channel, the Co- or the Cross (X)- Polarization channel [3],[9],[11]. This paper applies the filtering principle to three possible polarimetric radar channels and compares the resultant imagery. The radar channels in consideration here are Co-Pol, X-Pol, and M-Polarization channels. Co-Pol means that the receiving antenna has the same polarization state as that of the transmitting antenna, X-Pol channel has the orthogonal polarization state relative to the transmitting antenna, whereas the M-Pol channel has an antenna whose polarization state is matched to the scattered wave on receiving. These channels can be synthesized by the principle of radar polarimetry. First, the principle of characteristic polarization imaging is outlined based on Stokes vector and Kennaugh matrix formulation because this approach holds both for completely polarized and for partially polarized wave cases. Then, using the definition of contrast enhancement factor, i.e., the power ratio of wanted target versus other target as a discriminator between two target classes, enhanced polarimetric images for these three channels are shown and compared using the NASA DC-8 AIRSAR data sets (CC0045L, Bonanza Creek, AK). It is shown that the optimally enhanced polarimetric Co-Pol and X-Pol channel imagery play a dominant role in imaging and that the polarization state which yields optimally enhanced image does not necessarily coincide with the one minimizing unwanted target power in the X-Pol channel.

Manuscript received May 8, 1995.
Manuscript revised August 11, 1995.

† The authors are with Niigata University, Niigata-shi, 950-21 Japan.
†† The author is with University of Illinois at Chicago, IL, 60607-7018, USA.
††† The author is with Korea Advanced Institute of Science and Technology, Taejon, 305-701 Korea.

2. Channel Power Expression

The polarization state of a completely polarized wave can be expressed by a 4×1 Stokes vector, which in terms of tilt angle τ and ellipticity angle ε is given as

$$\boldsymbol{g} = \begin{bmatrix} g_0 \\ g_1 \\ g_2 \\ g_3 \end{bmatrix} = \begin{bmatrix} g_0 \\ g_0 \cos 2\tau \cos 2\varepsilon \\ g_0 \sin 2\tau \cos 2\varepsilon \\ g_0 \sin 2\varepsilon \end{bmatrix} \tag{1}$$

where g_0 is the total power carried by the wave. The tilt angle τ and ellipticity angle ε are geometric parameters of an elliptic polarization state and are in the range of $-45° \le \varepsilon \le 45°$, $-90° \le \tau \le 90°$, respectively. The relation of these parameters and the Stokes vector are illustrated on the Poincaré sphere in Fig.1. Any polarization state is specified on a point on the Poincaré sphere, and there is a one-to-one correspondence between all possible polarization states and points.

Now, let's assume that the radar has three channel modes for operation as shown in Fig.2, i.e., Co-Pol, X-Pol,

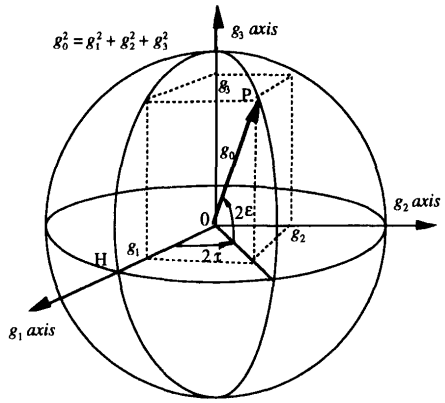

Fig.1 Stokes vector and geometric parameters relation on the Poincaré Sphere.

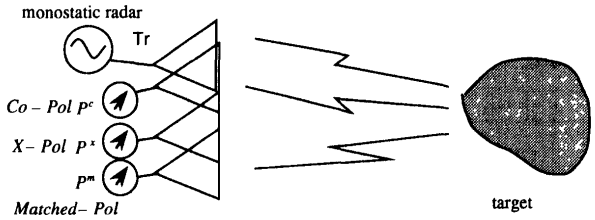

Fig.2 Three polarimetric radar channels.

and M-Pol channel configurations. In polarimetric radar operation, what we can obtain is the polarimetric scattering characteristics of target. This scattering nature can be measured in a orthogonal polarization basis such as H-V polarization combination. Since we are interested in polarimetric information, we assume that the transmitted wave $\boldsymbol{g}_t$ has a unit magnitude and is completely polarized,

$$g_0^2 = g_1^2 + g_2^2 + g_3^2 = 1 \quad . \tag{2}$$

If the polarimetric scattering nature of target is measured in 4× 4 real Mueller or Kennaugh matrices, the power for each channel is given [14], [15] as

(a) Co-Pol

$$P^c = \frac{1}{2}\boldsymbol{g}_t^{\mathrm{T}}[K]_c\boldsymbol{g}_t \tag{3}$$

$$[K]_c = \begin{bmatrix} 1 & 0 & 0 & 0 \\ 0 & 1 & 0 & 0 \\ 0 & 0 & 1 & 0 \\ 0 & 0 & 0 & -1 \end{bmatrix}[M] \tag{4}$$

where the superscript T denotes transpose,

(b) X-Pol

$$P^x = \frac{1}{2}\boldsymbol{g}_t^{\mathrm{T}}[K]_x\boldsymbol{g}_t \tag{5}$$

$$[K]_x = \begin{bmatrix} 1 & 0 & 0 & 0 \\ 0 & -1 & 0 & 0 \\ 0 & 0 & -1 & 0 \\ 0 & 0 & 0 & 1 \end{bmatrix}[M] \tag{6}$$

(c) Matched-Pol

$$P^m = \boldsymbol{g}_t^{\mathrm{T}}[K]_m\boldsymbol{g}_t \tag{7}$$

$$[K]_m = \begin{bmatrix} 1 & 0 & 0 & 0 \\ 0 & 0 & 0 & 0 \\ 0 & 0 & 0 & 0 \\ 0 & 0 & 0 & 0 \end{bmatrix}[M] = \frac{1}{2}[K]_c + \frac{1}{2}[K]_x \tag{8}$$

where [K] is the Kennaugh matrix and [M] is the Mueller matrix. The reason why we adopted this formulation is due to the fact that a reflected wave from natural distributed target in general becomes partially polarized wave (completely polarized component plus depolarized component) even if a completely polarized wave is transmitted and that these two matrices hold both for completely polarized case and for partially polarized case. The degree of polarization is included in [K] and [M]. Appendix gives the relation of Kennaugh matrix and Sinclair scattering matrix elements for the completely polarized case. The power expressions (3), (5), (7) omit a proportionality factor, which is a function of transmitting power, path length, antenna gain, and wavelength. The Matched Pol channel receives the total power of the scattered wave, which is the sum of Co-Pol channel and X-Pol channel. Although both matrices [K] and [M] represent scattering properties of a radar target, it should be noted that Mueller matrix is defined such that the origin of coordinate system of the scattered wave is taken on the target, whereas Kennaugh matrix case the origin of coordinate system is taken on the radar (see chap.7 of [16]). In the backscattering case which we treat in the NASA DC-8 AIRSAR data, the Kennaugh matrix formulation is preferable.

3. Polarimetric Imaging Methodology

It is possible to produce any polarimetric channel image by choosing a polarization state of the transmitter. There would be infinite number of polarimetric imagery because the number of polarization state is infinite as anticipated in Fig.1.

If a Kennaugh matrix is given for one pixel or a specific target in a polarimetric SAR imagery, it is possible to optimize the radar channel power as a function of $\boldsymbol{g}_t$. The polarization states which yield stationary points in the radar channel power signature are called the characteristic

polarization states. It is known [4] that there exists physically a total of eight distinct characteristic polarization states for a target. These characteristic polarization states are subject to target, incidence angle, aspect angle, etc. If we choose a specific $\boldsymbol{g}_t$ among eight characteristic polarization states for one target, say Co-Pol Maximum, then it becomes possible to re-calculate all pixel powers again according to the power expressions with $\boldsymbol{g}_t$, which results in the Co-Pol Max image for the target. This methodology is referred to as characteristic polarization filtering technique, and this kind of techniques cannot be performed without a full polarimetric SAR data. The polarimetric filtering technique has advantages such that the target is maximized in the scene while the other is weakened and the polarization state itself provides some polarimetric information on the target which may be useful for target identification or classification.

4. Polarimetric Contrast Enhancement in Radar Channel

The power expression applies to every pixel, in other words, it applies to any point in an entire scene. SAR imagery usually consists of thousands of pixels. There exist many discrete targets as well as speckle noise inherent to SAR imagery. Sometimes we need to discern the details of a specific target within a complex featured scene against undesired background images or against noise. In this case, discrimination of a target or optimization of one target against the other becomes important. This requirement leads to a target enhancement technique which is different from the characteristic polarization filtering in the previous section. As a discriminator between two target classes, let's define a contrast enhancement factor as the ratio of power of wanted target versus power of other target to be compared with:

$$C = \frac{\text{power of wanted target}}{\text{power of other target}} \tag{9}$$

which leads to the following expression for

(a) Co - Pol channel

$$C_c = \frac{P_1^c}{P_2^c} = \frac{\boldsymbol{g}_t^{\mathrm{T}} [K]_{c,1} \boldsymbol{g}_t}{\boldsymbol{g}_t^{\mathrm{T}} [K]_{c,2} \boldsymbol{g}_t} \tag{10}$$

(b) X - Pol channel

$$C_x = \frac{P_1^x}{P_2^x} = \frac{\boldsymbol{g}_t^{\mathrm{T}} [K]_{x,1} \boldsymbol{g}_t}{\boldsymbol{g}_t^{\mathrm{T}} [K]_{x,2} \boldsymbol{g}_t} \tag{11}$$

(c) Matched - Pol channel

$$C_m = \frac{P_1^m}{P_2^m} = \frac{\boldsymbol{g}_t^{\mathrm{T}} [K]_{m,1} \boldsymbol{g}_t}{\boldsymbol{g}_t^{\mathrm{T}} [K]_{m,2} \boldsymbol{g}_t} \tag{12}$$

where $[K]_1$ represents the Kennaugh matrix for which we wish to maximize the received power by changing the components of $\boldsymbol{g}_t$, and $[K]_2$ is the one to be minimized. Using the formulation of enhancement factors, we examined how the polarimetric contrast behaves in the image for each radar channel.

The problem here is to find a polarization state which optimizes the enhancement factors. The variable is the transmitting polarization state $\boldsymbol{g}_t$. There exists no closed-form analytical method for solving the optimal polarization state for Eqs.(10)-(12). Some trials [7]-[11] have been carried out to solve for the enhancement factor, however, they still employ a numerical method at the final stage. Therefore, we employed a numerical approach for finding the optimal polarization state from the outset.

The data set analyzed is a full polarimetric scene of Bonanza Creek, AK, USA, which has been acquired with the NASA AIRSAR system (data set no.CC0045L) on March 19, 1988. It consists of a set of 1024 pixel × 750 line data and is stored in an equivalent Mueller matrix form, but different from those of (A3) in Appendix. Each pixel (resolution) represents an area echo of 7.5 m (in range direction) × 11 m (along flight direction) measured at L band with the wavelength 24 cm. The selected area contains a forested area and wet land regions (river side) for which we wish to enhance the image of the river side. This is accomplished by maximizing the polarimetric power densities pertaining to the pixel sets of the river side versus minimizing those pertaining to the forest. For this purpose, we have selected several pixels within river side and forested area. The number of chosen pixels in each area was 42 for river side and 36 for forest. These numbers were determined by typical polarization characteristics as shown in Fig.3.

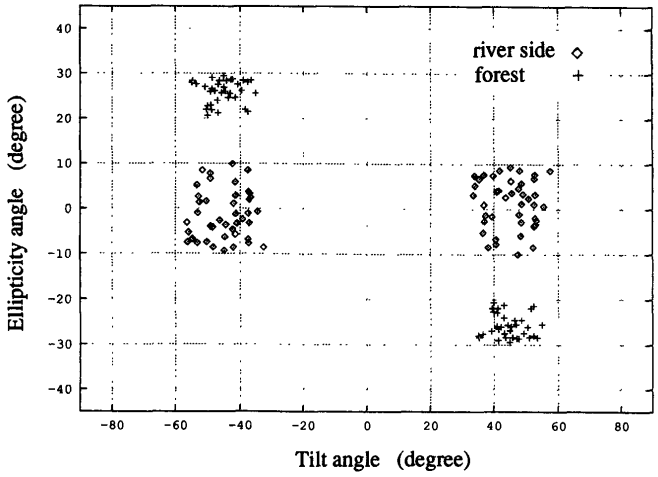

Fig.3 Distribution of X-Pol Max Polarization state for river side and forest.

Figure 3 shows a distribution of the X-Pol Max polarization state for each region as a function of tilt and ellipcity angles. The Kennaugh matrices of these two areas were averaged and found to be:

River side

$$[K]_1 = \begin{bmatrix} 2.5903 & 0.3716 & 0.0391 & 0.0060 \\ 0.3716 & 2.0150 & 0.0426 & -0.0274 \\ 0.0391 & 0.0426 & -0.9294 & -0.1669 \\ 0.0060 & -0.0274 & -0.1669 & 1.5047 \end{bmatrix},$$

Forested area

$$[K]_2 = \begin{bmatrix} 1.2749 & 0.3539 & -0.0614 & -0.0298 \\ 0.3539 & 1.0870 & -0.0007 & 0.0010 \\ -0.0614 & -0.0007 & 0.3154 & 0.7949 \\ -0.0298 & 0.0010 & 0.7949 & -0.1276 \end{bmatrix}.$$

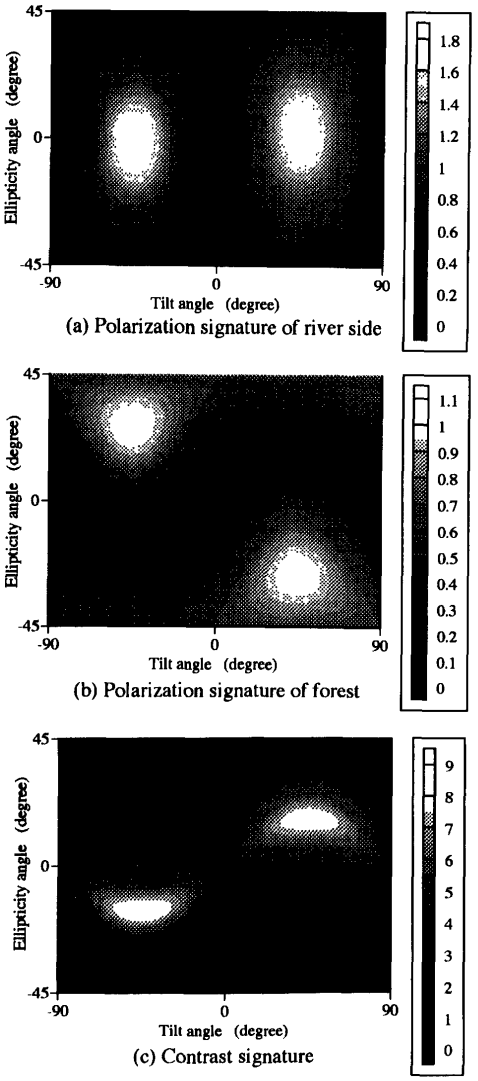

(a) Polarization signature of river side

(b) Polarization signature of forest

(c) Contrast signature

Fig.4 Power and contrast signatures in the X-Pol channel.

It is now possible to determine the polarimetric response of these two targets. Polarimetric power densities and contrast enhancement factor signatures for the X-Pol channel case are shown in Fig.4. It should be noted in Fig.4(*a*) and (*c*) that a polarization state which maximizes the radar return for one specific target is different from the one which maximizes the contrast ratio of (11). The maximum contrast (two white points in (*c*)) is achieved around the X-Pol Saddle polarization states (two corresponding positions of (*c*) in (*b*)) for the forested area. It is interesting to note in this case that the X-Pol Saddle yields the maximum contrast rather than the X-Pol Min. This shows that the maximum of (11) is not achieved by minimizing the denominator of (11). This point is different from the completely polarized wave case where a polarization state yielding the maximum contrast is equal to the polarization state minimizing the unwanted other target. The polarization states which give the maximum contrast enhancement factors, together with the X-Pol Max and Min polarization states for the river side, are listed in Table 1.

Table 1 Polarization state and contrast in the X-Pol channel.

Pol. state			Stokes Vector			Contrast
	ε	τ	g_1	g_2	g_3	
Max. for river side	1.9	45.4	-0.0137	0.9976	0.0679	4.1247
	-1.9	-44.6	0.0137	-0.9976	-0.0679	
Min. for forest	0.0	90.0	-1.0000	0.0000	0.0000	3.0628
	0.0	0.0	1.0000	0.0000	0.0000	
Maximum Contrast	16.4	45.8	-0.0235	0.8402	0.5417	8.0906
	-16.4	-44.2	0.0235	-0.8402	-0.5417	

(a) X-Pol image which maximizes river side

(b) Maximum contrast image (river side / forest)

Fig.5 Polarimetric filtered images in the X-Pol channel.

The polarimetric enhanced images using these polarization states are shown in Fig.5. It is seen that the maximum contrast enhanced image (*b*) is superior to the X-Pol Max image (*a*). This superiority can also be confirmed by comparing the value of contrast enhancement factor in Table 1. In addition, the boundary of river and river side becomes apparent in this maximum contrast image (*b*). It is understood that the image contrast is strongly dependent on the polarization state.

A similar procedure was repeated to the Co-Pol channel and the M-Pol channel cases. The results are shown in Figs.6-9, and in Table 2 and 3. The polarization state which gives the maximum contrast is close to the polarization state which minimizes the unwanted power, i.e., Co-Pol Min or

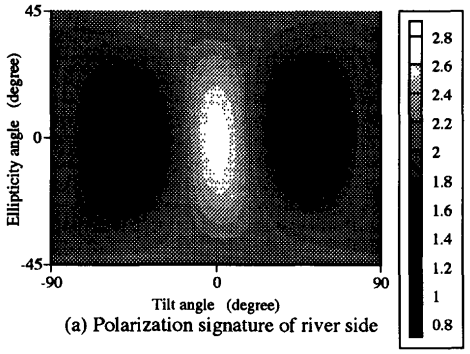

(a) Polarization signature of river side

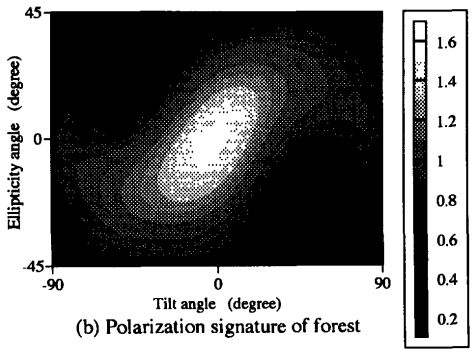

(b) Polarization signature of forest

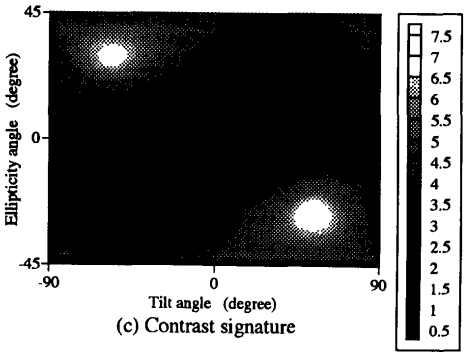

(c) Contrast signature

Fig.6 Power and contrast signatures in the Co-Pol channel.

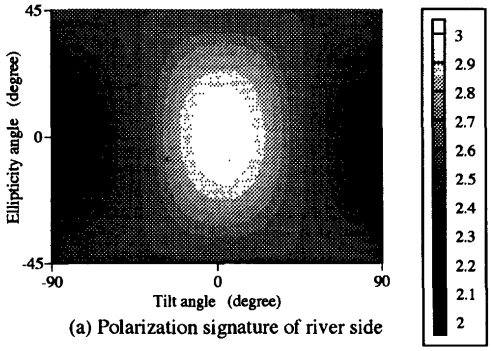

(a) Polarization signature of river side

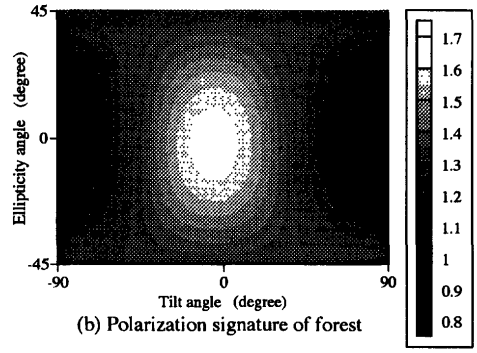

(b) Polarization signature of forest

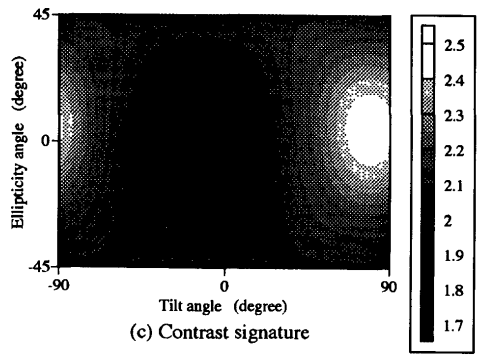

(c) Contrast signature

Fig.8 Power and contrast signatures in the M-Pol channel.

(a) Co-Pol image which maximizes river side

(b) Maximum contrast image (river side / forest)

Fig.7 Polarimetric filtered images in the Co-Pol channel.

Table 2 Polarization state and contrast in the Co-Pol channel.

Pol. state			Stokes Vector			Contrast
	ε	τ	g_1	g_2	g_3	
Max. for river side	-0.8	0.7	0.9993	0.0244	-0.0279	1.7458
Min. for forest	-24.6	53.6	-0.1932	0.6242	-0.7570	7.1744
Maximum Contrast	-27.0	53.8	-0.1777	0.5603	-0.8090	7.3860

(a) M-Pol image which maximizes river side

(b) Maximum contrast image (river side / forest)

Fig.9 Polarimetric filtered images in the M-Pol channel.

M-Pol Min of the unwanted target. It is seen in Fig.7 that the forested area appears much darker in the maximally enhanced image (*b*) than that in the Co-Pol Max image (*a*). It is possible to see the details (distribution of black color) within the forested areas in this enhanced images Figs.5(*b*) and 7(*b*) although the power from the forest area is minimized. This is one of contrast enhancements in a reverse sense that we can see the minimum power (black color) distribution within a scene rather than in the maximum power (white color) distribution in an enhanced contrast image.

5. Comparison of Three Channel Imagery

As can be seen in Figs. 5, 7, and 9, the image contrast is strongly dependent on polarization state in the X- and Co-Pol channels than in the M-Pol channel. This fact is due to the scattering characteristics difference by polarization. The image qualities (contrast) in the X-Pol and Co-Pol channels were almost the same in this example. However, for the case of M-Pol channel, the polarization change does not provide

Table 3 Polarization state and contrast in the M-Pol channel.

Pol. state			Stokes Vector			Contrast
	ε	τ	g_1	g_2	g_3	
Max. for river side	0.5	3.0	0.9944	0.1045	0.0175	1.8297
Min. for forest	2.4	85.1	-0.9820	0.1696	0.0837	2.4412
Maximum Contrast	4.2	79.5	-0.9236	0.3545	0.1461	2.4534

Table 4 Average power in three channel imagery.

	Co-Pol	X-Pol	M-Pol
Horizontal	1.0000	0.1426	1.1427
Vertical	0.7335	0.1426	0.8761
45 degree Linear	0.5355	0.4778	1.0133
135 degree Linear	0.5278	0.4778	1.0056
Left Handed Circular	0.6278	0.3890	1.0177
Right Handed Circular	0.6084	0.3890	1.0012

significant change in the image contrast. This is because the M-Pol channel power is the sum of Co-Pol and X-Pol powers and hence the dynamic range in the power variation on pixel to pixel becomes small. Although we have chosen specific targets in this paper, these are typical natural objects, i.e., non man-made objects. Therefore it is understood that the polarimetric enhanced X-Pol and Co-Pol channel images play a dominant role in imaging in a complex featured background rather than the M-Pol image.

Various polarimetric channel images can be obtained based on Eqs. (3), (5), and (7) by choosing a polarization state. For a qualitative comparison of three channel images, we examined average power densities over the entire scene of Bonannza Creek as a function of polarization state. Since there exists an infinite number of polarization states, we employed some typical polarization states to calculate the power according to (3), (5), and (7). For the sake of comparison, all power densities in these three channels are normalized by the power density of the Co-Pol channel with linear horizontal polarization. The result is listed in Table 4. It is seen that the M-Pol channel gives the largest power density because the channel receives all the energy of the scattered wave on receiving. For the case of X-Pol channel, the averaged power densities are always less than that of the Co-Pol channel power. The X-Pol power achieves its maximum around 45 and 135 degree linear polarizations for this scene. From inspection of various specific polarimetric images (CM0045, CM0117, CM1077), it is observed that the image brightness (power) and the contrast are strongly

dependent on the polarimetric channel and the transmitting and the receiving polarization states.

6. Conclusion

Three polarimetric channel images are illustrated to show how the polarization plays in SAR imagery using NASA JPL DC-8 AIRSAR data sets. By using the definition of polarimetric contrast enhancement factor and characteristic polarization states, we examined image quality and/or contrast with respect to transmitter polarization state. Two target categories (river side and forest) within a SAR image were selected for enhancement procedure. It is shown that a minimum polarization state which gives minimum power for unwanted target does not necessarily yields the maximum contrast in the X-Pol channel image. This fact is different from the result in the completely polarized wave case where the minimum polarization state always provides the maximum contrast regardless of radar channel. The maximum contrast polarization state in the Co-Pol and M-Pol channel was close to the polarization state which minimized the undesired power. However, the M-Pol channel does not provide high contrast because it always receives the total sum of reflected power resulting in a flatter contrast signature than those of the Co- and X-Pol channels.

The maximum polarization states (Co-Pol and X-Pol maxs) for a specific target do not provide maximum contrast or high quality image in complex featured background radar scenes.

The average power was calculated to show the difference in radar channel as a function of typical polarization states. The M-Pol channel always yielded the brightest image, the Co-Pol channel provides the second brightest, and the X-Pol the third. The polarimetric enhanced Co-Pol and X-Pol channel images play a dominant role in imaging and retrieving information (such as distribution information) on specific targets.

Acknowledgments

Authors are grateful to Mr. Takashi Yamada and Hideyuki Watanabe, the former student of Niigata University who initially contributed to this research, and to Dr. Anthony Freeman at CAL-TECH/JPL who has provided the data sets together with a visualization software. The data format conversion was carried out by Mr. Mikio Aoyama at Software Division, Fujitsu Co. Ltd.

References

[1] A. B. Kostinski and W.-M. Boerner, "On foundation of radar polarimetry," IEEE Trans. Antennas & Propag., vol.AP-34, no.12, pp.1395-1403, Dec. 1986.

[2] J. J. Van Zyl, H. A. Zebker, and C. Elach, "Imaging radar polarization signatures: theory and observation," Radio Sci., vol.22, no.4, pp.529-543, 1987.

[3] H. A. Zebker, Van Zyl, and D. N. Held, "Imaging radar polarimetry from wave synthesis," J. of Geophysical Res., vol.92, no.B1, pp.683-701, Jan. 1987.

[4] W.-M. Boerner et al. ed., "Direct and Inverse Methods in Radar Polarimetry," Part 1 and 2, Kluwer Academic Publishers, Netherlands, 1992.

[5] A. B. Kostinski, D. J. Brian, and W.-M. Boerner, "Optimal reception of partially polarized waves," J. of Opt. Soc. Am., A, vol.5, no.1, pp.58-64, Jan. 1988.

[6] A. B. Kostinski, D. J. Brian, and W.-M. Boerner, "Polarimetric matched filter for coherent imaging," Canadian J. of Physics, vol.66, p.871, Oct. 1988.

[7] W.-M. Boerner, M. Walter, and A. C. Segal, "The concept of the polarimetric matched signal & image filters," EARSeL Advances in Remote Sensing, vol.2, no.1-I, pp.219-252, 1993.

[8] M. Tanaka, "Optimum antenna polarizations in partially polarized scattering," Proc. of ISNCR '89, Kyoto Japan, pp.496-501, 1989.

[9] M. Tanaka and W.-M. Boerner, "Optimum antenna polarizations for polarimetric contrast enhancement," Proc. of ISAP'92, Sapporo Japan, vol.2, pp.545-548, 1992.

[10] J. J. Van Zyl, "Unsupervised classification of scattering behavior using imaging radar polarimetry data," IEEE Trans. Geosci. & Remote Sensing, vol.27, no.1, pp.36-45, Jan. 1989.

[11] P. C. Dubois and J. J. Van Zyl, "Polarization filtering of SAR data," in Direct and Inverse Methods in Radar Polarimetry, Part 2, pp.1411-1424, Kluwer Academic Publishers, Netherlands, 1992.

[12] R. Touzi, T. L. Toan, A. Lopes, and E. Mougin, "Polarimetric discriminators for SAR images," IEEE Trans. Geosci. & Remote Sensing, vol.30, no.5, pp.973-980, Sept. 1992

[13] A. A. Swartz, H. A. Yueh, J. A. Kong, L. M. Novak, and R. T. Shin, "Optimal polarizations for achieving maximum contrast in radar images," J. of Geophysical Research, vol.93, no. B12, pp.15252-15260, 1988.

[14] Y. Yamaguchi, K. Sasagawa, M. Sengoku, and T. Abe, "Derivation of characteristic polarization states for partially polarized waves," Proc. IEICE Spring Conf'90, B-159, March 1990.

[15] W. L. Yan and W.-M. Boerner, "Optimal polarization states determination of the Stokes reflection matrices [M_p] for the coherent case, and of the Mueller matrix [M] for the partially polarized case," J. Electromagnetic Waves and Appl., vol.5, no.10, pp.1123-1150, Oct. 1990.

[16] H. Mott, "Antennas for Radar and Communications," John Wiley & Sons, pp.415-419, 1992.

[17] J. J. Van Zyl, C. H. Papas, and C. Elachi, "On the optimum polarization of incoherently reflected waves," IEEE Trans. Antennas & Propag., vol.AP-35, no.7, pp.818-825, 1987.

[18] A. B. Kostinski, B. D. James, and W.-M. Boerner, "On the polarimetric contrast optimization," IEEE Trans. Antennas & Propag., vol.AP-35, no.8, pp.988-991, 1987.

[19] Y. Yamaguchi, T. Yamada, H. Watanabe, M. Sengoku, and W.-M. Boerner, "Polarimetric radar channel image and its enhancement using NASA JPL AIRSAR data," IEICE Technical Report, A·P93-34, May 1993.

Appendix : Relation of Matrices Elements

For a completely polarized wave and for the backscattering case, the elements of $[K]_c$ are related to the elements of Sinclair scattering matrix $[S]$ as

$$[K]_c = \begin{bmatrix} 1 & 0 & 0 & 0 \\ 0 & 1 & 0 & 0 \\ 0 & 0 & 1 & 0 \\ 0 & 0 & 0 & -1 \end{bmatrix} [M] = \begin{bmatrix} m_{00} & m_{01} & m_{02} & m_{03} \\ m_{01} & m_{11} & m_{12} & m_{13} \\ m_{02} & m_{12} & m_{22} & m_{23} \\ m_{03} & m_{13} & m_{23} & -m_{33} \end{bmatrix} \quad (A \cdot 1)$$

$$[S] = \begin{bmatrix} S_{xx} & S_{xy} \\ S_{yx} & S_{yy} \end{bmatrix} \quad (A \cdot 2)$$

$$m_{00} = \frac{1}{2}\left(|S_{xx}|^2 + 2|S_{xy}|^2 + |S_{yy}|^2 \right) \quad (A \cdot 3a)$$

$$m_{01} = m_{10} = \frac{1}{2}\left(|S_{xx}|^2 - |S_{yy}|^2 \right) \quad (A \cdot 3b)$$

$$m_{02} = m_{20} = \mathrm{Re}\left(S_{xx} S_{xy}^* + S_{xy} S_{yy}^* \right) \quad (A \cdot 3c)$$

$$m_{03} = -m_{30} = \mathrm{Im}\left(S_{xx} S_{xy}^* + S_{xy} S_{yy}^* \right) \quad (A \cdot 3d)$$

$$m_{11} = \frac{1}{2}\left(|S_{xx}|^2 - 2|S_{xy}|^2 + |S_{yy}|^2 \right) \quad (A \cdot 3e)$$

$$m_{12} = m_{21} = \mathrm{Re}\left(S_{xx} S_{xy}^* - S_{xy} S_{yy}^* \right) \quad (A \cdot 3f)$$

$$m_{13} = -m_{31} = \mathrm{Im}\left(S_{xx} S_{xy}^* - S_{xy} S_{yy}^* \right) \quad (A \cdot 3g)$$

$$m_{22} = \mathrm{Re}\left(S_{xx} S_{yy}^* \right) + |S_{xy}|^2 \quad (A \cdot 3h)$$

$$m_{23} = -m_{32} = \mathrm{Im}\left(S_{xx} S_{yy}^* \right) \quad (A \cdot 3i)$$

$$-m_{33} = |S_{xy}|^2 - \mathrm{Re}\left(S_{xx} S_{yy}^* \right) \quad (A \cdot 3j)$$

Care should be taken about the sign of these elements in the power calculation†.

† References by JPL [17], [10], etc. are based on a different formulation of Stokes vector, resulting in a Stokes matrix different from the definition of Kennaugh matrix [16].

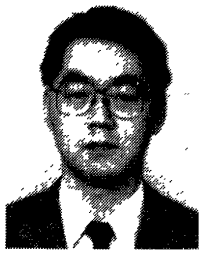

Yoshio Yamaguchi received the B. E. degree in electronics engineering from Niigata University in 1976, and the M. E. and Dr. Eng. degrees from Tokyo Institute Technology in 1978 and 1983, respectively. In 1978, he joined the Faculty of Engineering, Niigata University, where he is now a Professor. From 1988 to 1989, he was a Research Associate at the University of Illinois, Chicago. His interests are in the field of propagation characteristics of electromagnetic waves in lossy medium, radar polarimetry, microwave remote sensing and imaging. Dr. Yamaguchi is a senior member of IEEE, and a member of the Japan Society for Snow Engineering.

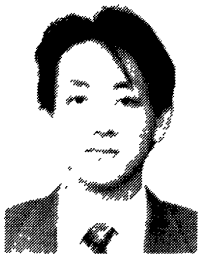

Yuji Takayanagi was born in Gumma Prefecture, Japan, on Oct. 16, 1970. He received the B. E. degree in Information Engineering from Niigata University, in 1994. He is now a graduate student pursuing his M. E. degree in Niigata University where he is engaged in radar polarimetry applied to remote sensing.

Wolfgang-M. Boerner received the Arbitur (B.S.) degree from the August on Platen Gymnasium, Ansbach, West Germany in 1958, his Dipl.Ing. (M.Sc.) degree from the Technische Universitat Munchen in 1963, and his Ph.D. degree from the Moore School of Electrical Engineering, The University of Pennsylvania, Philadelphia in 1967. From 1967 to 1968 he was a Research Assistant Engineer at the University of Michigan, MI. In 1968 he joined the University of Manitoba, Canada. Since 1978 he has been a Professor at the Department of Electrical Engineering and Computer Science, University of Illinois at Chicago, and Director of the Communications and Sensing Laboratory. He is a fellow of the IEEE, and a member of the Canadian Association of Physicists, Sigma XI, the Society of Photo-Optical Instrumentation Engineers, the Optical Society of America, the Society of Exploration Geophysicists, the Society of Engineering Sciences, the American Association for the Advancement of Science, the Fulbright Alumni Association, and the U.S. Commissions B, C, and F of the International Scientific Radio Union.

Hyo Joon Eom received the B.S. degree in electronic engineering form Seoul National University, Korea, and M.S. and Ph.D. degrees in electrical engineering form the University of Kansas, Lawrence, in 1977 and 1982, respectively. Form 1981 to 1984, he was a research associate at the Remote Sensing Laboratory of the University of Kansas. Form 1984 to 1989, he was with the faculty of the Department of Electrical Engineering and Computer Science, University of Illinois at Chicago. He joined the Department of Electrical Engineering, Korea Advanced Institute of Science and Technology in 1989 as an Associate Professor, where he is a Professor. His research interests are electromagnetic theory, radar remote sensing and wave scattering.

Masakazu Sengoku received the B. E. degree in electrical engineering from Niigata University, Japan, in 1967 and the M. E. and Ph. D. degrees from Hokkaido University in 1969 and 1972, respectively.In 1972, he joined the staff at Hokkaido University as a Research Associate. In 1978, he was an Associate Professor at Niigata University, where he is presently a Professor. During 1986-1987, he was a Visiting Professor at the University of California, Berkeley, and at the University of Illinois, Chicago. His research interests include transmission of information, network theory, and graph theory. He is a recipient of the best paper award of IEICE in 1992. Dr. Sengoku is a senior member of the IEEE of Japan, and a member of Japan Society for Industrial and Applied Mathematics.